

NEW UPDATED RESULTS OF PALEOMAGNETIC DATING OF CAVE DEPOSITS EXPOSED IN ZA HÁJOVNOU CAVE, JAVOŘÍČKO KARST

JAROSLAV KADLEC

Institute of Geophysics AS CR, v.v.i., Boční II/1401, 141 01 Prague 4, the Czech Republic; e-mail: kadlec@ig.cas.cz

KRISTÝNA ČÍŽKOVÁ

Institute of Geology AS CR, v.v.i., Rozvojová 135, 165 02 Prague 6, the Czech Republic; e-mail: cizkovak@gli.cas.cz

STANISLAV ŠLECHTA

Institute of Geology AS CR, v.v.i., Rozvojová 135, 165 02 Prague 6, the Czech Republic; e-mail: slechta@gli.cas.cz



Kadlec J., Čížková, K., Šlechta, S. (2014): New updated results of paleomagnetic dating of cave deposits exposed in Za Hájojnou Cave, Javoříčko Karst. – Acta Mus. Nat. Pragae, Ser. B, Hist. Nat, 70(1-2): 27–34, Praha. ISSN 1804-6479.

Abstract. Clastic cave deposits exposed in Za Hájojnou Cave in Javoříčko Karst were recently dated using a superconducting rock magnetometer device. Normal polarities identified in the upper portion of the sedimentary fill are interpreted as a normal Brunhes Chron imprint (sediments are younger than 781 ka). The sediments in the lower portions of the sequence reveal reversed or transition polarities which could be interpreted as a Matuyama Chron imprint (sediments are older than 781 ka). In the current research, the sediment magnetic fabric was assessed based on anisotropy of magnetic susceptibility. The sediment magnetic fabric was controlled by local water flow combined with cavity morphology.

■ Javoříčko Karst, Za Hájojnou Cave, Early and Middle Pleistocene, paleomagnetic dating.

Received January 20, 2014

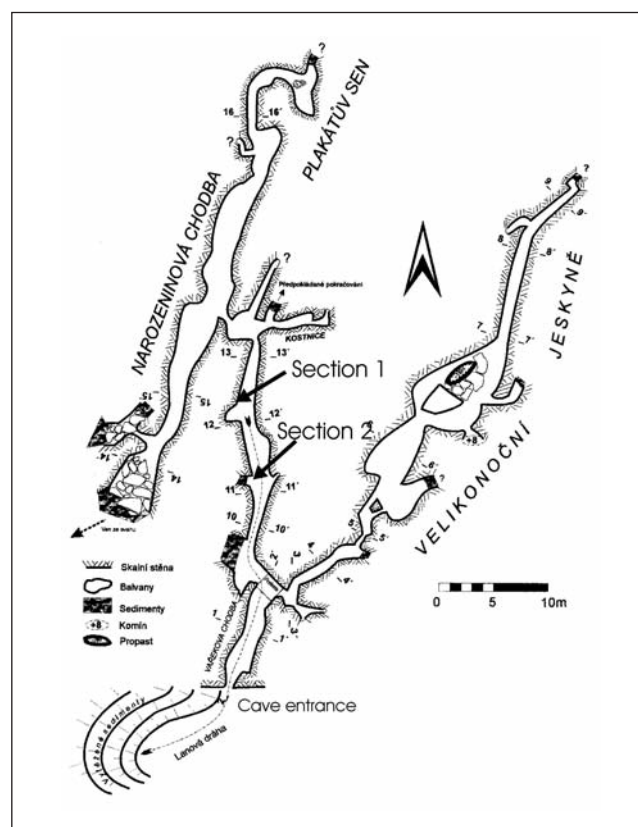
Issued October, 2014

Introduction

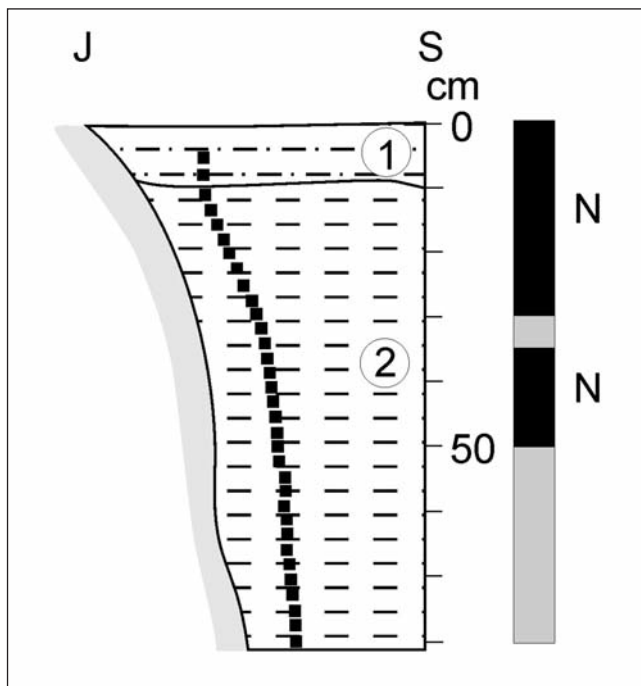
Preliminary results of the magnetostratigraphic study of Cave deposits exposed in Za Hájojnou Cave conducted between 2001–2004 did not provide totally satisfactory conclusions. The main reason was low stability of the direction of detrital remanent magnetization (DRM). In many cases, data measured on a spinner magnetometer JR-5A (AGICO Ltd.) did not allow for satisfactory interpretation of paleomagnetic polarities preserved in sediments from the time they were deposited (Kadlec et al. 2005). For this reason, we decided to repeat the paleomagnetic analysis using a more sensitive, and for unconsolidated sediments a much more suitable, superconducting rock magnetometer 2G – model 760R (SRM) completed with an alternating field demagnetizing unit developed by 2G Enterprises. This device has been housed in the Paleomagnetic laboratory of the Institute of Geology AS CR, v.v.i. since 2007.

Geological settings

Two sedimentary sections were analyzed in the Za Hájojnou Cave. The first section (Section No. 1) is situated in the Vykopaná chodba (= Excavated Corridor) about 28 m from the Cave entrance (Text-fig. 1). The second sedimentary section (Section No. 2) is located in an excavated vertical space below the Vykopaná chodba. Section No. 1 is above and partially overlaps Section No. 2. Bed Nos. 1 and 2 in



Text-fig. 1. Map of the Za Hájojnou Cave with Section Nos. 1 and 2 (surveyed by M. Vaněk, status in 2005).



Text-fig. 2. Cave deposits exposed in Section No. 1 and recorded paleomagnetic polarities. 1 – clayey silt, brown with white clasts; 2 – clayey silt to silty clay, brown. Geomagnetic polarity scale: black (N) – normal polarities, grey – intermediate or uninterpretable polarities. For more details see text.

Section No. 1 (Text-fig. 2) correspond with bed Nos. 4 and 5 in the original, older Section 1 in the Kostnice II (= Charnel-house II) (investigated during the research campaign conducted between 2001–2004 (Kadlec et al. 2005). Current resampling of Section 1 in the Kostnice II was not possible because of partial excavation of sediments since 2004.

Method used

Magnetic fabric analysis

The magnetic fabric of the sediments can be analyzed using the anisotropy of magnetic susceptibility (AMS) approach. The AMS reflects the preferred orientation of magnetic minerals and can be used for texture interpretation in sedimentary rocks. Magnetic anisotropy can be visualized using an ellipsoid with three perpendicular principal axes $k_1 > k_2 > k_3$. The maximum axis (k_1) is denoted as magnetic lineation and the plane perpendicular to the minimum axis (k_3) defines magnetic foliation. The AMS ellipsoid magnitude can be presented as the k_1/k_3 ratio, known as the degree of anisotropy, P (Nagata 1961). The AMS ellipsoid shape can be described by the shape parameter T (Jelinek 1981). Oblate shapes correspond to $0 < T \leq 1$, prolate shapes correspond to $-1 \leq T < 0$. The degree and shape of the AMS depend on the lithology and compaction imposed on the deposit. If a rock is deposited in a current, magnetic foliation may be imbricated, dipping at an angle of $< 15^\circ$ in the direction opposite to the flow direction. Magnetic lineation is either parallel to the flow direction or, in the case of high current velocity, perpendicular to it (Tarling and Hrouda 1993). The original bedding-parallel fabric of sedimentary rocks is later

enhanced by the effect of diagenetic compaction from overburden pressure and the expulsion of pore fluids. The degree and shape of anisotropy depends on the lithology and compaction imposed on the rock. Oriented samples of clastic cave deposits were collected in plastic boxes (volume 6.7 cm^3). Low-field magnetic susceptibility (MS) and AMS were measured on a KLY-4 Kappagridge device (Jelinek 1973).

Paleomagnetic analysis

Oriented samples of sediments were demagnetized on the SRM device using an alternating field (AF) in 12 to 14 steps from a natural state up to 80 mT. The obtained data was processed using Kirschvink (1980) multi-component analysis. The results are produced as paleomagnetic polarities of discrete samples and declination and inclination mean directions calculated using Fisher (1953) statistics.

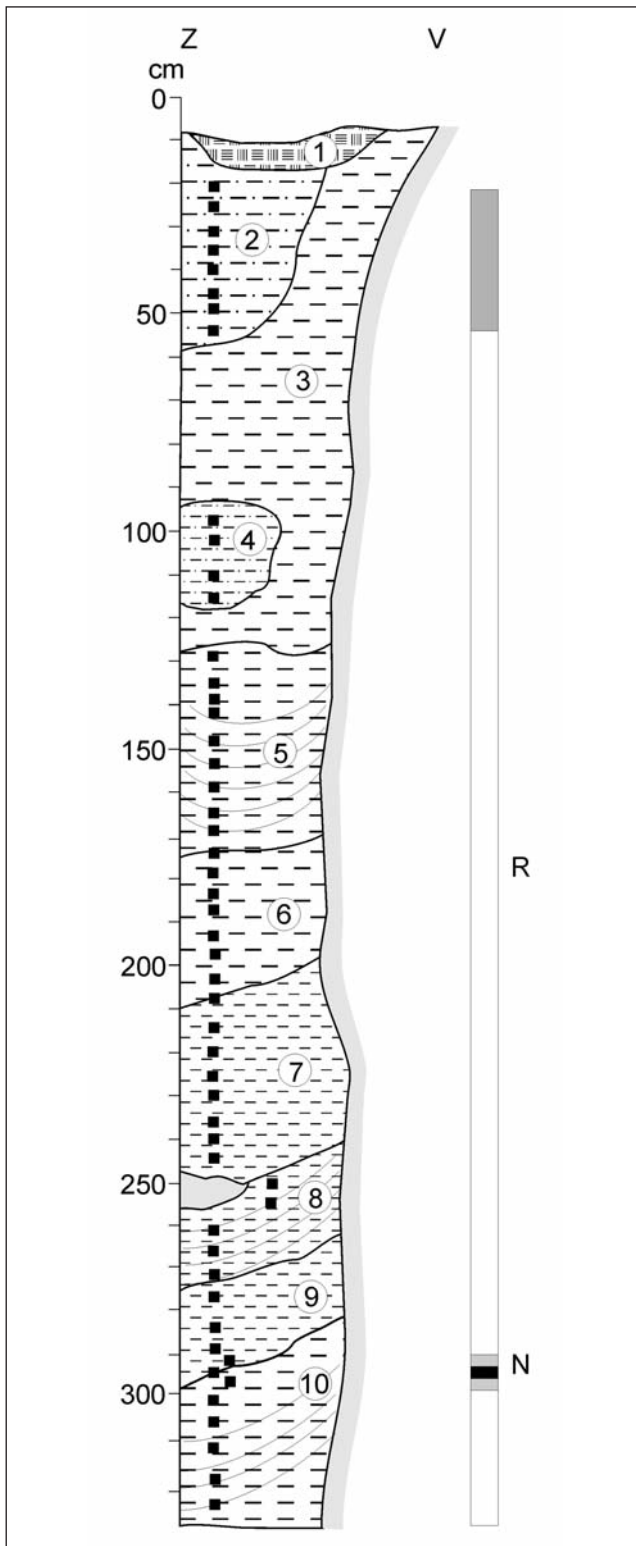
Description of sedimentary sections

Section No. 1

Brown clayey silt with abundant white angular clasts of weathered limestone and bone fragments (size up to 4 mm) is exposed in the upper portion of the section (Bed No. 1 in Text-fig. 2). The remaining lower portion of the section consists of brown silty clay without white clasts (Bed No. 2). Neither of the beds show any noticeable stratification. These two beds correspond with bed Nos. 4 and 5 in the Kostnice II section investigated between 2001–2004 (Kadlec et al. 2005).

Section No. 2

The youngest bed, Bed No.1, reworked during the spelunker excavations, is underlain by brown massive clayey silt with abundant rusty stains with black dots colored by manganese oxides (Bed No. 2 in Text-fig. 3). Bed No. 3 is formed by chaotically deposited brown clayey silt to silty clay again with abundant rusty stains, black dots and coatings on crack faces. This bed represents the younger sediment fill of erosional space created by water running along a cave wall. Carbonate cemented lenses of the clastic sediment lying parallel with the cave wall occasionally occur in the lower part of the bed. Underlying Bed No. 4 consists of massive grey silty clay. Bed No. 5 is formed from light brown laminated clayey silt with dark coatings along the crack faces. The lighter and more silty undulating laminae are 1–4 mm thick, other darker and more clayed laminae are up to 10 mm thick. Underlying Bed No. 6 is formed from structureless brown clayey silt to clay. Light brown massive clayey silt to clay form Bed No. 7, which is underlain by brown silty clay with abundant light dots of weathered limestone clasts up to 10 mm in size and dipping to the W at an angle less than 40° (Bed No. 8). Bed No. 9 appears as clayey sandy silt with abundant light erosional clay fragments less than 4 cm in size. Similar sediment is exposed in the base of Bed No. 10. The only difference is that the lower bed with laminae dipping to the W contains less clay fragments than Bed No. 9.



Text-fig. 3. Cave deposits exposed in Section No. 2 and recorded paleomagnetic polarities. 1 – reworked deposits; 2 – clayey silt, light brown with abundant black dots, structureless; 3 – clayey silt to silty clay, brown, chaotically deposited; 4 – clayey silt, light brown, structureless; 5 – clayey silt, light brown, laminated; 6 – clayey silt to silty clay, brown, structureless; 7 – clayey silt to silty clay, light brown, structureless; 8 – clayey silt, brown with abundant white carbonate clasts; 9 – clayey sandy silt, brown with abundant lighter clayey fragments; 10 – clayey sandy silt, brown with sporadic lighter clayey fragments. Geomagnetic polarity scale: black (N) – normal polarities, white (R) – reversed polarities, grey – intermediate or uninterpretable polarities. For more details see text.

Results

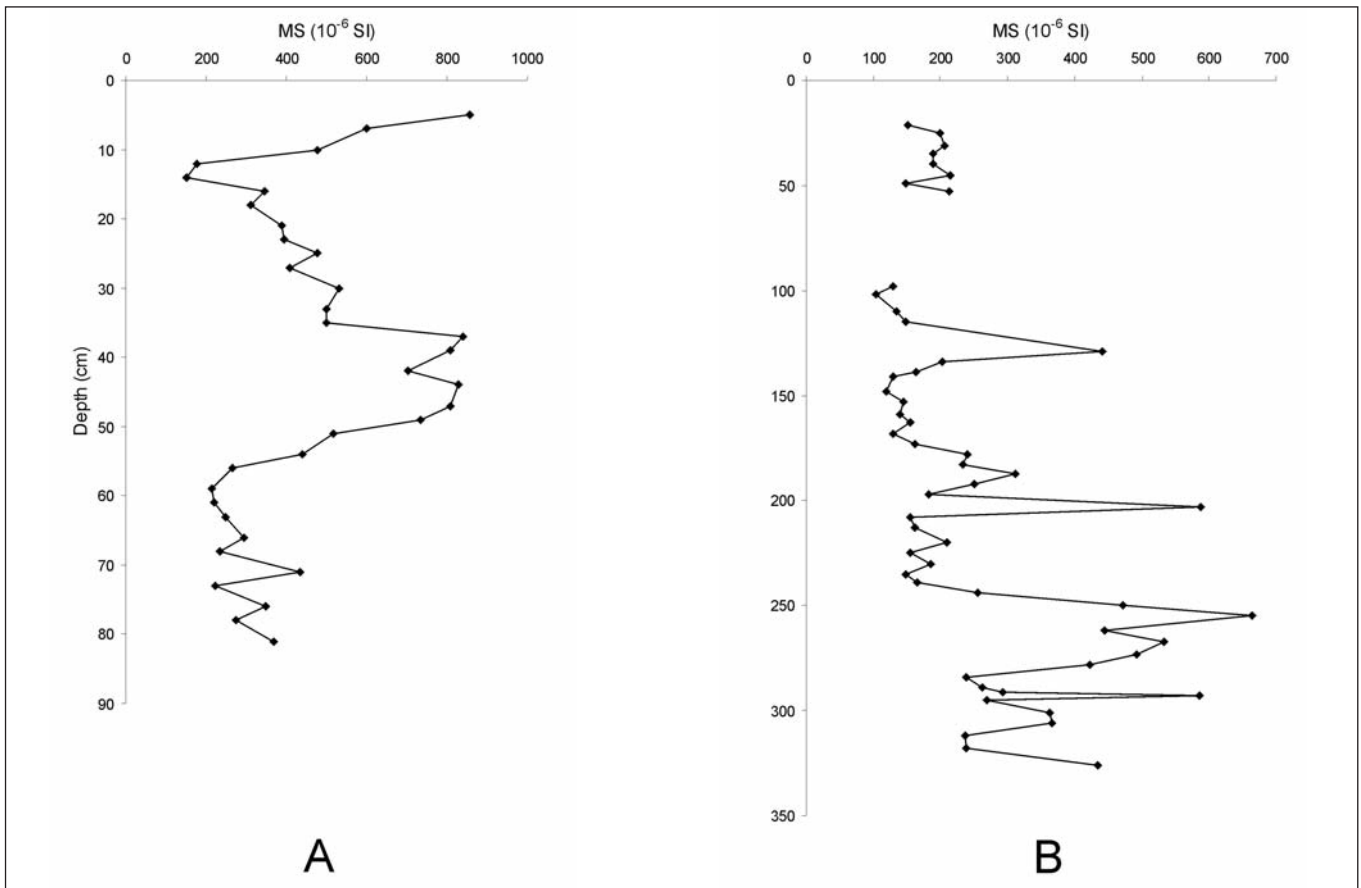
The MS values ranged between 150 and 858 (10^{-6} SI) in Section No. 1 and between 105 and 664 (10^{-6} SI) in Section No. 2 (Text-fig. 4). Sediments in Section No. 1 showed a low AMS degree ($\leq 8.2\%$, graph bottom left in Text-fig. 5). The AMS degree increased with rising MS values in most samples. The AMS ellipsoid revealed an oblate shape with only one exception (Sample No. 68). The axis directions of the AMS ellipsoid demonstrate anomalous magnetic fabric with magnetic foliation dipping to the N at an angle less than 40° . Magnetic lineation follows an ENE-WSW direction (Text-fig. 6). In Section No. 2 the magnetic foliation slightly dips to the NW and the magnetic lineation shows the same trend.

Natural remanent magnetization (NRM) intensity in the natural state (NS) fluctuates between 1.95 and 35.26 mA/m in Section No. 1, and between 0.21 and 18.52 mA/m in Section No. 2. The upper part of Section No. 1 (Samples Nos. 7–49) mostly show normal DRM polarities. The underlying sediments record intermediate polarities (Samples Nos. 51–81, see Tab. 1). The upper part of Section No. 2 shows intermediate or uninterpretable DRM polarities (Samples Nos. 21–53). The underlying sediments show reversed polarities (see Tab. 1). The only exception is sample No. 293 showing normal polarity. Unfortunately, neighboring samples could not be reliably interpreted as supporting this normal polarity interpretation. The mean directions of paleomagnetic declination and inclination are shown in Text-fig. 7. The mean direction of declination with normal polarity (16 samples) is 337° and the mean angle of inclination is 48° . The samples with reversed polarities (27 samples) reveal a mean declination direction of 201° and inclination angle of -49° . Examples of the demagnetization process of samples with normal and reversed polarities are shown in Text-figs. 8 and 9.

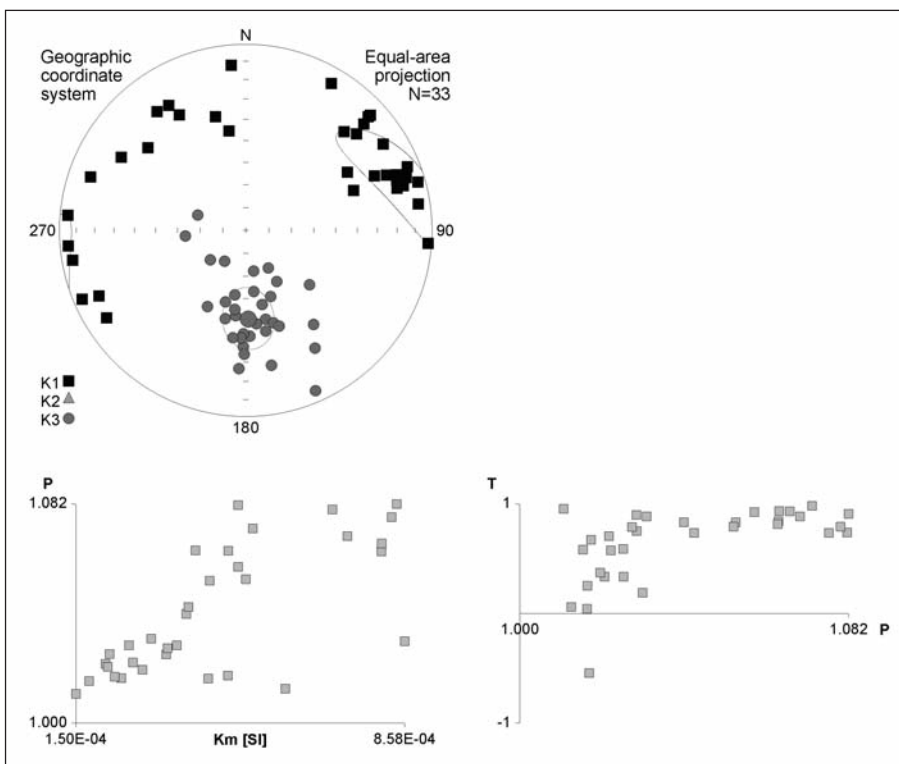
Discussion of results

Sediment magnetic fabric in Section No. 1 is strongly affected by water running from N to S through the cave passage. The limestone thresholds across the passage bottom could probably act as a vertical barrier for the water flow. Magnetic fabric in Section No. 2 is influenced by a narrow vertical space which controlled sediment deposition. Lamination of the sediments dip to the W in the section, the same as the magnetic lineation and foliation.

Paleomagnetic polarity interpretation for the upper part of Section No. 1 produce the same result (normal polarities) as the older research campaign carried out between 2001–2004 (Kadlec et al. 2005). The sediments are younger than 781 ka (Brunhes/Matuyama boundary) and were most likely deposited during the beginning of the Middle Pleistocene which is supported by paleontological content in the overlaying debris layers (Musil et al. 2005). Radiometric dating of flowstone layers intercalated into the limestone debris also supports this interpretation (Lundberg et al. 2014). The intermediate or uninterpretable polarities revealed in the underlying samples can be explained by sediment deposition during a period when the Earth's magnetic field polarity



Text-fig. 4. Bulk magnetic susceptibility values in deposits exposed in the Section Nos. 1(A) and 2 (B).



Text-fig. 5. Anisotropy of magnetic susceptibility in deposits exposed in Section No. 1. Circular diagram – projection of the longest k_1 axes (squares) and the shortest k_3 (circles) of the AMS ellipsoid to the lower projection hemisphere, the larger square and circle show intermediate direction of the k_1 axis and k_3 axis, respectively. Lines represent reliability ellipses of the k_1 and k_3 axis. Lower left diagram – AMS degree (P) versus bulk MS (Km); right left diagram – AMS shape (T) versus AMS degree (P).

changed, or due to overprinting of the primary DRM record by post-deposition formation of minerals able to carry the younger DRM record (for example goethite). The presence

of such a mineral with characteristic high coercivity would cause a low AF demagnetization ability to be detected in some samples. The reversed DRM polarities detected in

Tab. 1. Natural remanent magnetization characteristics of sediments exposed in Section No. 1

Sample (cm) – sample depth in the section; MS – magnetic susceptibility; M – natural state magnetization; polarity: N – normal, R – reversed, N-R, R-N – transitional, ? - impossible interpretation; D – interpreted magnetic declination; I – interpreted magnetic inclination; MAD - maximum angular deviation.

sample (cm)	MS (10 ⁻⁶ SI)	M (mA/m)	polarity	D (°)	I (°)	MAD
5	858	35.26	?			
7	601	14.04	N	13.5	68.1	2.1
10	478	10.56	N	358.9	57.8	2.7
12	178	2.55	N	356.3	54.6	2.4
14	150	1.95	N	358.7	44.6	2.7
16	345	7.97	N	4.7	55	3.7
18	312	7.82	N	339.9	44.5	7.2
21	388	8.20	N	346.4	41.6	5.6
23	393	11.27	N	331.8	37.5	4.8
25	478	14.77	N	338.9	33.1	9.2
27	408	9.46	N	331.4	31.5	10.3
30	531	10.46	?			
33	499	9.82	?			
35	500	11.65	?			
37	841	27.01	N	324.6	54.5	3.9
39	808	27.59	N	339.8	53.5	4.4
42	703	23.12	N	327	42.6	7.2
44	830	30.03	N	320.5	49.4	6.8
47	809	28.67	N	319	45.5	10.2
49	735	28.45	N	318.8	28.6	11.4
51	516	9.91	R-N	277.4	-33.3	2.1
54	439	8.41	R-N	278	-38.4	5.3
56	265	4.97	R-N	277.1	-20	2.9
59	214	4.50	R-N	303.6	-0.8	1.5
61	219	4.33	R-N	297.9	-13.7	1.4
63	248	4.55	R-N	290.8	-19.7	0.8
66	293	7.21	R-N	334.5	-37.9	2.6
68	234	5.52	R-N	281.1	-30.2	1.8
71	435	15.33	R-N	295.1	-11.6	1.8
73	223	4.07	R-N	299.2	-55.2	1.8
76	348	7.14	R-N	301.5	-15.3	0.9
78	273	3.87	R-N	295.6	-49.3	1.9
81	368	7.36	R-N	302.2	-44.3	1.9

Section No. 2 indicate the age of the sediments as greater than 781 ka. The question remains if the normal polarity of sample No. 293 could represent the normal Jaramillo Subchron dated between 1070 and 990 ka BP (Gradstein et al. 2012). On the other hand, it is unlikely that an only 2 cm thick horizon could represent a period that lasted 80 ka. The second possible explanation is an erosion reduction of the upper part of an originally thicker horizon. The possibility of erosion is supported by the presence of clay fragments in Bed No. 9.

Conclusions

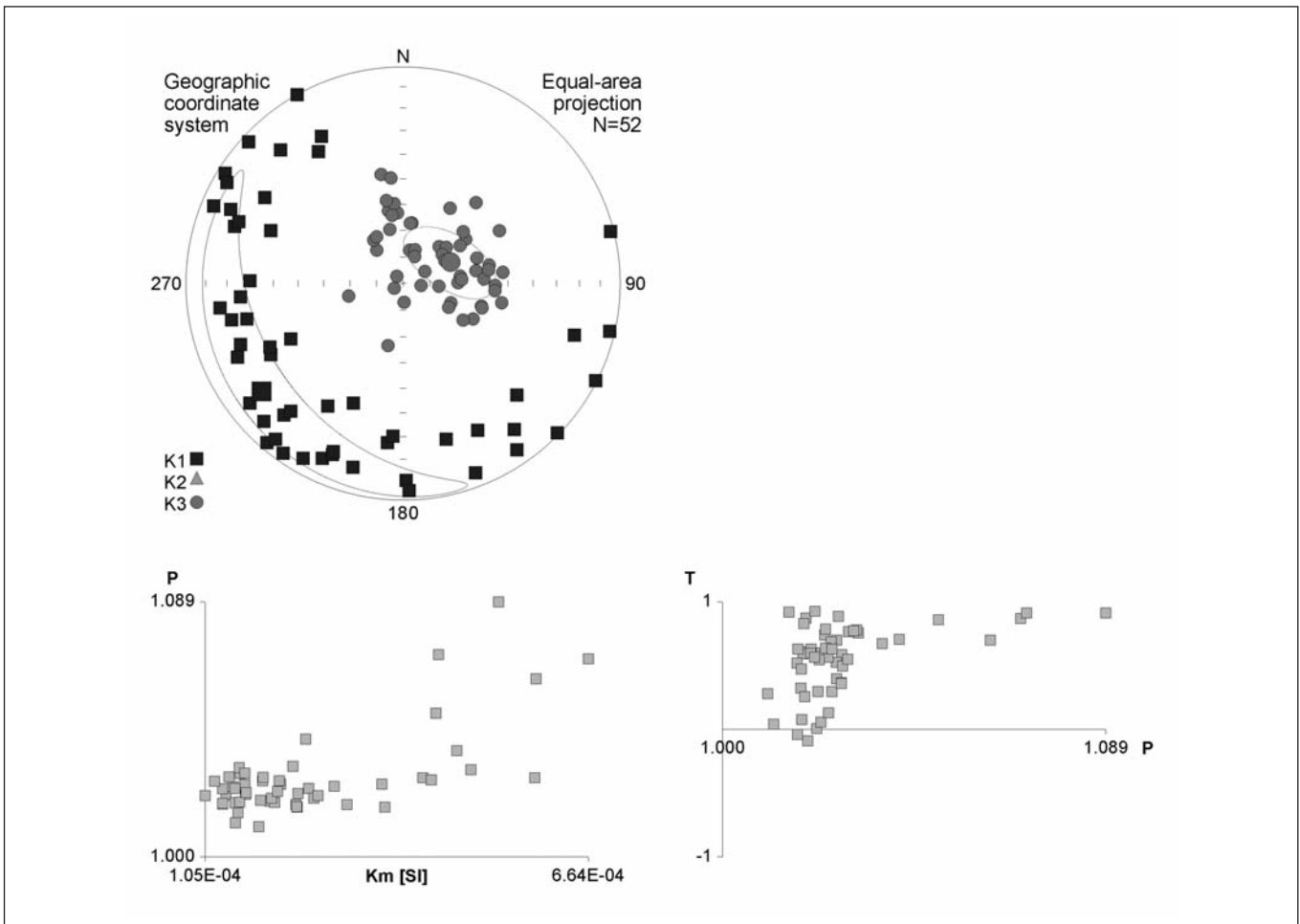
According to the recorded DRM paleomagnetic polarities, it is most probable that the clastic sediments exposed in the Za Hájovnou Cave, Section Nos. 1 and 2, were deposited during the Early Pleistocene and at the beginning of the Middle Pleistocene.

Tab. 2. Natural remanent magnetization characteristics of sediments exposed in Section No. 2

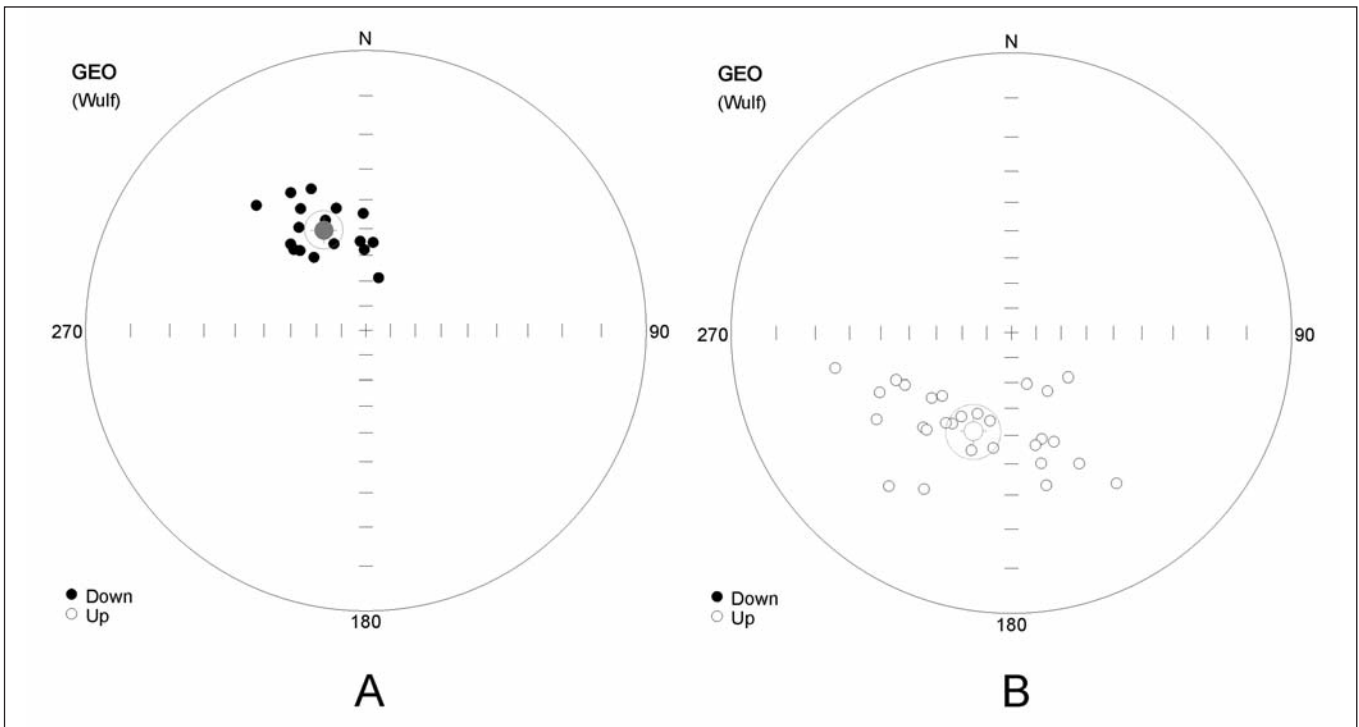
For explanation see Tab. 1.

sample (cm)	MS (10 ⁻⁶ SI)	M (mA/m)	polarity	D (°)	I (°)	MAD
21	152	0.83	N-R	137	22.2	3.5
25	200	2.35	?			
31	206	1.61	R	163.1	-68.6	4.9
35	189	1.40	N-R	70.2	26	5.3
40	189	1.66	R-N	136.5	-2.5	4.6
45	215	2.53	R-N	161.4	0	5.4
49	149	1.05	?			
53	213	1.92	?			
98	130	0.61	R	193.7	-54.4	10.4
102	105	0.21	R	209.3	-25	8.7
110	135	0.37	R	202.9	-55.5	2.9
115	148	0.40	R	213.2	-47.9	6.6
129	441	9.55	R?	120.7	-15.5	1.8
134	202	1.91	R	164	-47.2	3.8
139	163	2.55	N-R	259.7	1.2	2.6
141	130	2.86	R-N	270.9	-15.9	1.2
148	119	1.85	N-R	258.1	19.1	2.7
153	145	2.57	R-N	272.7	-5.2	3.3
159	139	4.84	N-R	252.3	4.6	1.3
163	156	9.60	R-N	246.6	-10	0.9
168	130	2.78	R-N	258.1	-17.7	1.5
173	162	3.41	N-R	258.9	2.9	1.6
178	240	4.24	N-R	228.5	13.3	2.7
183	233	1.69	R	145	-23.7	4.8
187	312	5.38	R	223.2	-40.6	12.5
192	251	2.57	R	247.8	-42.1	4.1
197	183	0.94	R	258.7	-24.7	3.7
203	587	11.79	R	218.7	-20.1	11.7
208	154	3.64	R	245.9	-35.5	2.6
213	162	4.27	R	237.5	-30.6	2.4
220	210	3.53	R	231	-49.8	1
225	155	2.97	R	227.9	-53.2	1.6
230	186	2.38	R	189	-45	1.1
235	148	3.29	R	221.3	-40.8	1.1
239	164	5.54	R	211	-51.8	1.5
244	256	5.51	R	216.2	-46.8	3.3
250	472	8.52	R	198.9	-42.4	4.8
255	664	15.29	?			
262	445	11.29	?			
267	533	13.93	?			
273	492	11.61	R	152.5	-34.7	4.1
278	422	9.77	?			
284	239	3.16	R	167.9	-45.6	6.4
289	263	3.92	R	167.1	-39.1	5.6
291	293	4.59	N-R	189.9	0.6	2.2
293	586	18.52	N	318.3	47.7	3.6
295	269	4.45	R-N	185.4	-20.4	3.5
301	362	8.84	R	148	-62.7	3.2
306	367	7.94	R	127.9	-61.2	6.5
312	237	2.66	R?	104.1	-24.6	4.1
318	238	5.02	R	158.6	-44.9	5.1
326	434	8.95	R	167.1	-31.8	4.1

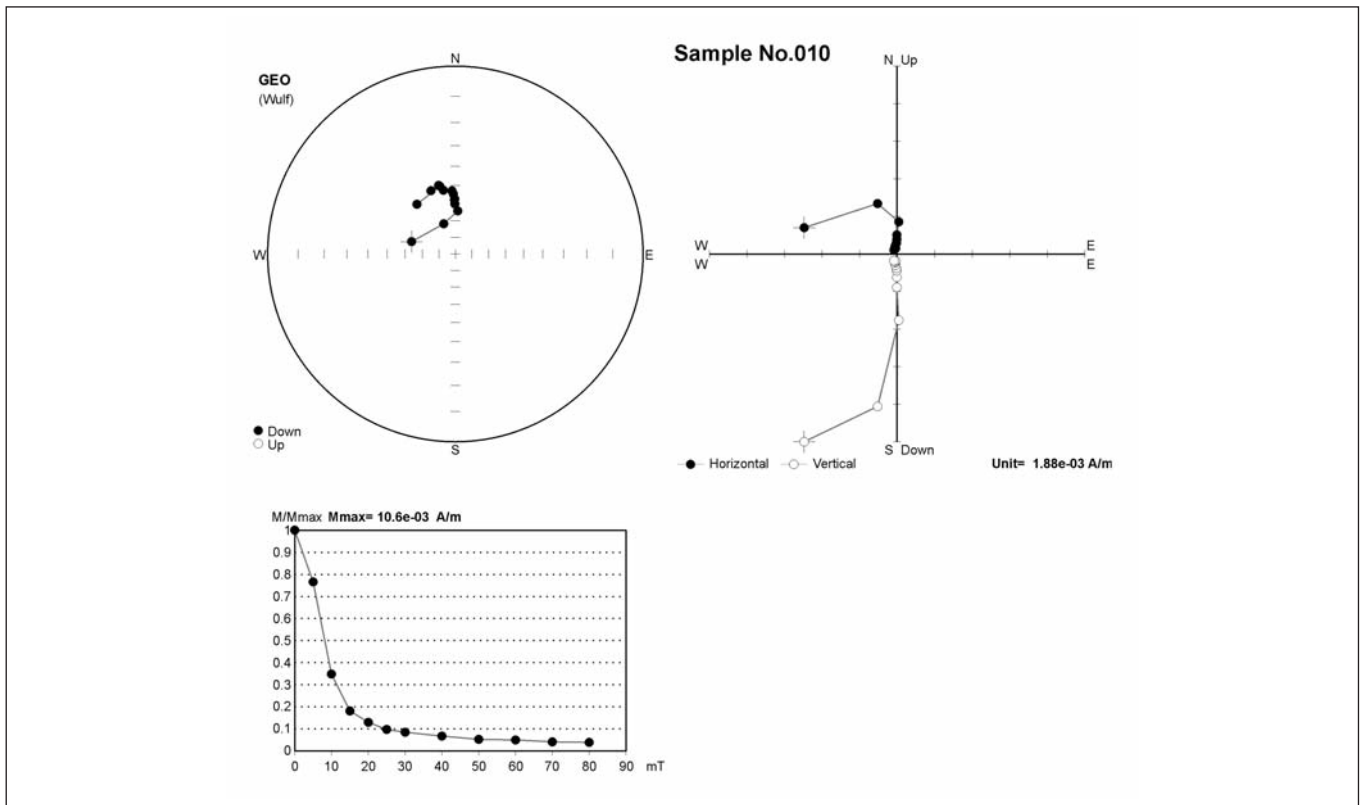
Even though the magnetic fabric of the sediments in both sections show the effect of local cave passage morphology on the deposition of sediments, this fact did not significantly affect the DRM polarity directions.



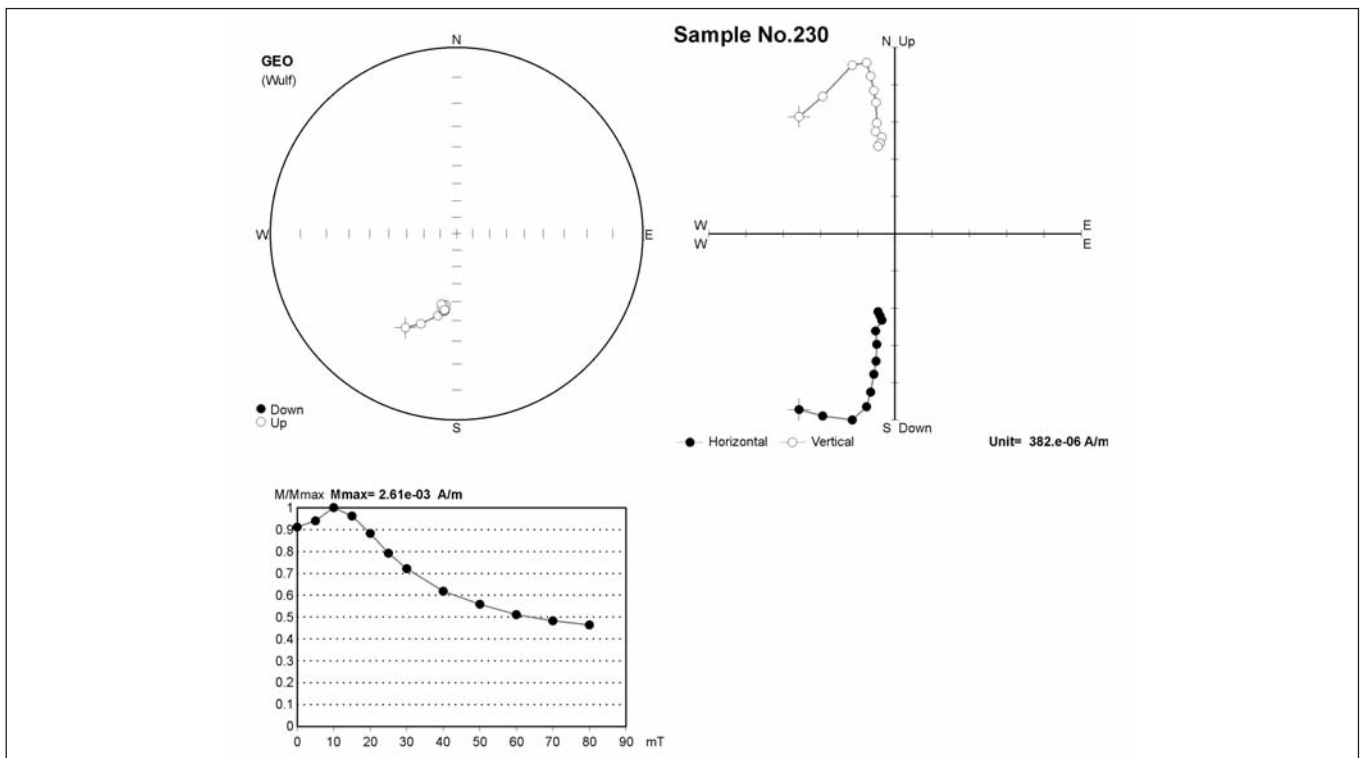
Text-fig. 6. Anisotropy of magnetic susceptibility in deposits exposed in Section No. 2. For explanation, see Text-fig. 5.



Text-fig. 7. Projection of the declinations and inclinations of primary component of the DRM vectors and a mean direction based on Fisher statistics A – samples with normal polarity (down - projection on the lower hemisphere), B – samples with reversed polarity (up - projection on the upper hemisphere).



Text-fig. 8. Alternating field demagnetization – Sample No. 010, Section No. 1 (normal polarity)
 Top left – DRM vector directions during demagnetization process, black circles - projection of vector directions to the lower hemisphere;
 top right - Zijderveld diagram, black circles - projection of vector directions into xy plane, white circles - projection of vector directions into xz plane;
 bottom left - normalized magnetization intensity values during the alternation field demagnetization.



Text-fig. 9. Alternating field demagnetization - sample No. 230, Section No. 2 (reversed polarity).
 Top left - DRM vector directions during demagnetization process, white circles - projection of vector directions to the upper hemisphere;
 top right - Zijderveld diagram, black circles - projection of vector directions into xy plane, white circles - projection of vector directions into xz plane;
 bottom left - normalised magnetization intensity values during the alternation field demagnetization.

Acknowledgements

The project was supported from the institutional funding provided by the Institute of Geology AS CR, v.v.i. No. RVO67985831.

References

- Fisher, R. (1953): Dispersion on a sphere. – Proceedings of the Royal Society of London, Series A, 217: 295–305. <http://dx.doi.org/10.1098/rspa.1953.0064>
- Gradstein, F. M., Ogg, J. G., Schmitz, M. D., Ogg, G. M. (eds) (2012): The Geologic Time Scale 201. Volume 2. – Elsevier, Oxford, Amsterdam, Waltham, pp. 437–1144.
- Jelínek, V. (1973): Precision A.C. bridge set for measuring magnetic susceptibility and its anisotropy. – *Studia Geophysica at Geodaetica*, 17: 36–48. <http://dx.doi.org/10.1007/BF01614027>
- Jelínek, V. (1981): Characterization of the magnetic fabric of rocks. – *Tectonophysics*, 79: T63–T67. [http://dx.doi.org/10.1016/0040-1951\(81\)90110-4](http://dx.doi.org/10.1016/0040-1951(81)90110-4)
- Kadlec, J., Chadima, M., Pruner, P., Schnabl, P. (2005): Paleomagnetické datování sedimentů v jeskyni „Za Hájovnou“ v Javoříčku – předběžné výsledky [Palaeomagnetic dating of sediments in the “Za Hájovnou” Cave, Javoříčko Karst, Moravia – preliminary results]. – *Přírodovědné studie Muzea Prostějovska*, 8: 75–82. (in Czech)
- Kirschvink, J. L. (1980): The least-squares line and plane and the analysis of palaeomagnetic data. – *Geophysical Journal International*, 62(3), 699–718. <http://dx.doi.org/10.1111/j.1365-246X.1980.tb02601.x>
- Nagata, T. (1961): *Rock Magnetism*. 2nd edition. – Maruzen, Tokyo, 360 pp.
- Lundberg, J., Musil, R., Sabol, M. (2013): Sedimentary history of Za Hájovnou Cave (Moravia, Czech Republic): A unique Middle Pleistocene palaeontological site. – *Quaternary International*, 339–340: 11–24. <http://dx.doi.org/10.1016/j.quaint.2013.04.006>
- Musil, R. (2005): Jeskyně „Za Hájovnou“, výjimečná lokalita Javoříšského krasu [Za Hájovnou Cave, exceptional locality of Javoříčko Karst, Moravia]. – *Přírodovědné studie Muzea Prostějovska*, 8: 9–42. (in Czech)
- Tarling, D. H., Hrouda, F. (1993): *The Magnetic Anisotropy of Rocks*. – Chapman and Hall, London, 217 pp.